Chapter 29 – In-situ Stress in the Western Canada Sedimentary Basin

Authors:
J.S. Bell - Geological Survey of Canada, Calgary
P.R. Price - National Energy Board, Calgary
P.J. McLellan - Shell Canada Ltd., Calgary

Introduction

This chapter summarizes the current understanding of the state of in-situ stress in the Western Canada Sedimentary Basin. The information compiled here includes specific in-situ stress measurements, interpretations of well logs, inferences from hydraulic fracture records, inferences from drilling procedures and well production behavior, and measurements of geological indicators. These data combine to give a coherent regional picture of principal stress orientations, but are not as successful in providing a comprehensive appreciation of stress magnitudes.

We use the term in-situ stress to refer to the present-day active natural stresses within the basin - in other words, how much and in what directions are the rocks being compressed at a specific location today? We are not concerned here with any stress regimes of the past, or paleostresses, which might be indicated by permanent changes in rock fabric (e.g., Hobbs and Talbot, 1966).

Buried sediments respond to pressure and temperature and to fluids that pass through them. For example, the effects of temperature in terms of organic metamorphism are widely recognized and studied; the changes initiated by migrating fluids underpin the fields of diagenesis and metamorphic petrology. Less attention has been paid to the effects of pressure. The importance of fluid pressures in determining the effective strength of rocks is addressed in structural geology and its role in the entrapment and production of hydrocarbons is recognized. However, rock pressure (stress) has often been regarded as a vertically-acting phenomenon, synonymous with the overburden load. Horizontal stresses are commonly tacitly assumed to be equal to the overburden stress, yet most rocks in sedimentary basins are not compressed isotropically. Geological evidence of past conditions, together with numerous contemporary measurements, clearly document that buried rocks are generally under anisotropic stress conditions, where the principal stresses are of different magnitudes. As this situation exists in the Western Canada Sedimentary Basin, many geological and petroleum engineering investigations would benefit from considering the contemporary stress regime.

Appreciation of the stress regime can help us understand the recent tectonic evolution of a basin. From an engineering standpoint, how a rock behaves mechanically is determined by its own inherent physical properties and by the stress field to which it is subject. In-situ stress information can predict in which directions production-enhancing hydraulic fractures will propagate, can suggest within which formations they are likely to be contained, and can determine the optimum orientation for inclined and horizontal wells. Thus, stress data are valuable for plannning how best to recover hydrocarbons from reservoirs.

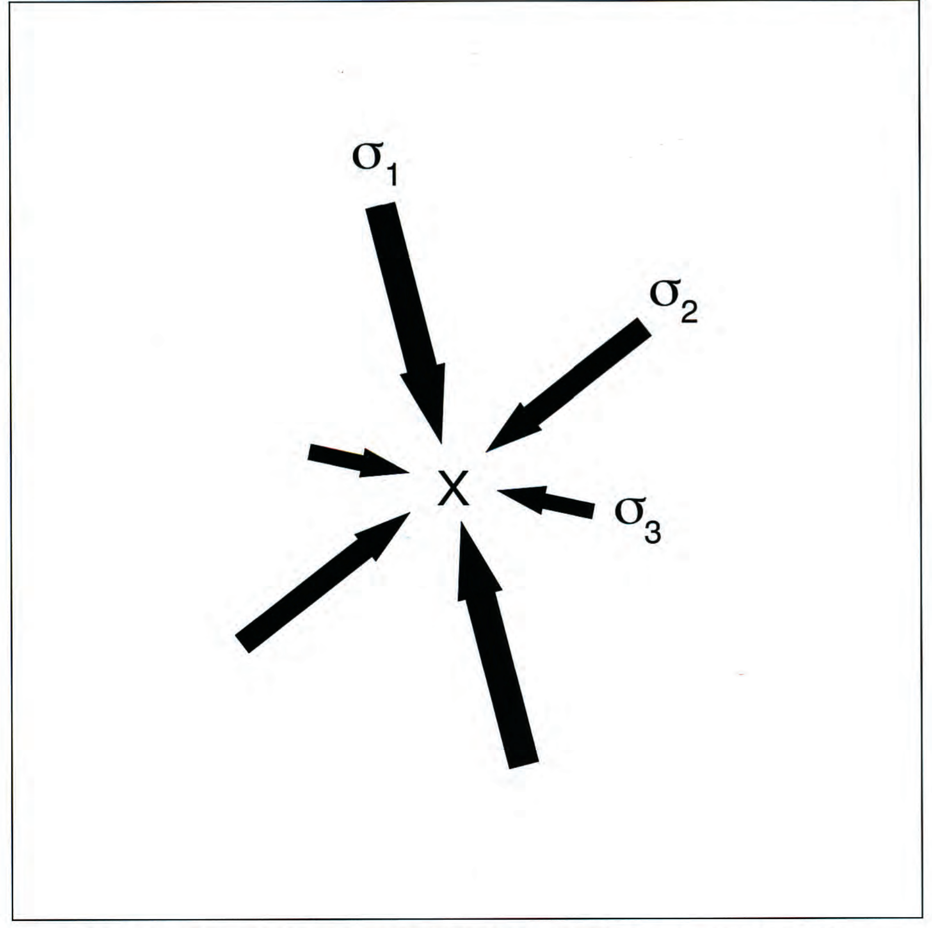

Figure 29.1 In-situ stresses at a point (x) in the subsurface, represented by three orthogonal principal stresses.

Principal Stresses

To fully describe the state of stress at a point in the subsurface, it is necessary to determine the magnitudes and orientations of three orthogonal principal stresses (Fig. 29.1), referred to as the largest, intermediate and smallest principal stresses. Stress is thus a tensor quantity (Jaeger and Cook, 1979). Consideration of a stress field is simplified if a "free surface" is present. This is a surface where the acting tangential forces are negligible, as occurs at the interface between the Earth's topographic surface and the atmosphere. One of the principal stresses will be oriented perpendicular to this interface, or "free surface". To a first order approximation, the present-day topography across the Western Canada Sedimentary Basin is horizontal, therefore one of the principal stresses will be close to vertical (Fig. 29.2). Even where there is some relief, its effect on deflecting stresses will be minimal below depths of a few hundred metres, so the generalization that one principal stress is vertical will hold (Hoek and Brown, 1980). If one principal stress is vertical, the other two principal stresses must be oriented horizontally. In this chapter, the vertical principal stress is referred to as S_V, and the larger and smaller horizontal principal stresses are designated S_{Hmax} and S_{Hmin} respectively (Fig. 29.2), and we use the convention that compression is positive.

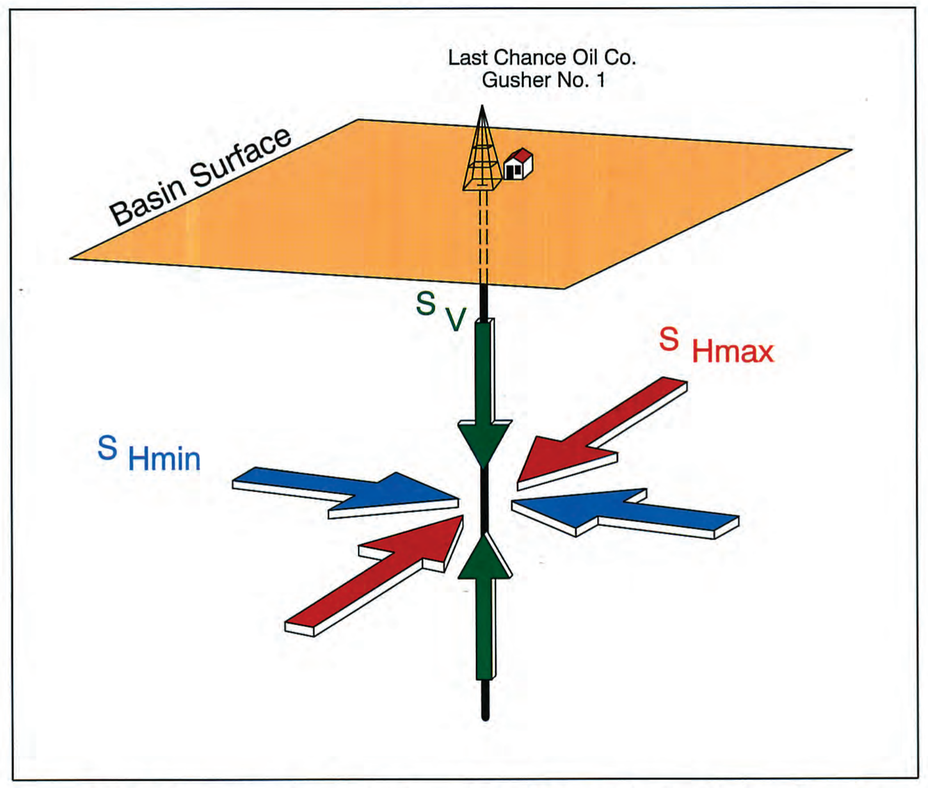

Figure 29.2 Assumed orientation of the principal stresses in the Western Canada Sedimentary Basin. The vertical principal stress, S_V is presumed to parallel vertical well bores; the other two orthogonal principal stresses would therefore be directed horizontally.

Stress Magnitude Measurements

Measurements and estimates of stress magnitudes at various locations within the Western Canada Sedimentary Basin are listed in Tables 29.1 and 29.2. These measurements and estimates have been obtained in the following ways. In some cases, the overburden pressure or vertical stress, S_V, was obtained by integrating a density log from surface to the depth of interest (e.g., Gronseth, 1990). In other cases, S_V was estimated assuming a mean density of 2400 kg/m³. This approximation was used because no direct measurements have yet been made of vertical stress at great depth in the Western Canada Sedimentary Basin. There are, however, two overcoring measurements of S_V that were made at shallow depth at the Kipp Mine in southern Alberta (Kaiser et al., 1982).

The smaller principal stress, S_{Hmin}, has been measured with accuracy by hydraulic micro-fracturing and by overcoring. Lower limits on its magnitude are provided by mini-frac tests, and upper limits have been estimated from selected formation leak-off tests.

The larger horizontal principal stress, S_{Hmax}, has been directly measured by overcoring methods at two sites in the Kipp Mine in southern Alberta (Kaiser et al., 1982). Elsewhere, it has been estimated from hydraulic fracture pressure data and pore pressure estimates using the following relation:

$$S_{Hmax} = S_{Hmin} - \text{Fracture Reopening Pressure} - \text{Pore Pressure}$$

This equation presumes that the rocks involved are relatively isotropic, impermeable, and exhibit linear elastic behaviour (Hubbert and Willis, 1957). For the hydraulic fracture cases, no other direct measurements of S_{Hmax} were made, hence there is no independent confirmation of these values.

The largest body of stress magnitude data in the Western Canada Sedimentary Basin comprises S_{Hmin} estimates that have been derived from several types of hydraulic fracturing tests, which have different levels of reliability.

The most reliable data come from measurements made by micro-fracture tests and by overcoring (Table 29.1, Figs. 29.3, 29.4). In the micro-fracture tests, hydraulically induced fractures were reopened several times until their closure pressures stabilized to give repeatable measures of S_{Hmin} (Kry and Gronseth, 1983; McLennan et al., 1982, 1986; McLellan, 1988a). The overcoring program involved precise monitoring of strain which, coupled with laboratory measurements of the geomechanical properties of the rocks involved, yielded reliable magnitudes of all three principal stresses (Kaiser et al., 1982). Both these techniques give accurate repeatable measurements of S_{Hmin}.

By contrast, mini-frac records and formation leak-off tests (Table 29.2) give less accurate estimates of S_{Hmin}. This is unfortunate, because the largest amount of potentially useful stress magnitude data for the Western Canada Sedimentary Basin is provided by these two sources. In earlier studies, the fracture closure stresses interpreted from mini-frac records were equated with S_{Hmin} (Woodland and Bell, 1989; Bell and McCallum, 1990). We now recognize that this procedure is rarely likely to give regionally representative values. Mini-fracs are performed to propagate small fractures in reservoirs that are candidates for subsequent larger acid or propped fracture treatments (massive fracs). The data gathered help design the final fracture treatments. In Alberta, reservoirs that are mini-fraced typically fall into two categories. They are either shallow oil sands or heavy-oil-bearing formations that are low to moderate producers, or they are deeper sandstone formations that may have already been produced successfully for some time and are now judged to need fracturing to boost their performance (McLellan, 1988b).

The shallow units (0-1200 m) with poor production expectations are, typically, fractured early in their production history before the virgin formation pressures have been reduced to any significant degree. On the other hand, by the time the deeper sandstone reservoirs (1200 m +) are fractured, they have usually been producing for some years, their fluid pressures have been reduced and, in some cases, sand has been produced, indicating that the reservoir

Table 29.1 Stress magnitudes measured by overcoring and micro-fracing in the Western Canada Sedimentary Basin.

Well or geographic site	Location shown on Fig. 29.7	Type of in-situ stress measurement method	Depth in metres below K.B.	S_{Hmin} in MPa	S_V in MPa	S_{Hmax} in MPa	Depth-normalized gradient of S_{Hmin} in kPa/m	Comments	Source
49.709°N, 112.935°W	Kipp Mine	Overcoring	152	3.0	3.6	4.3	19.7	All stresses measured	Kaiser et al., 1982
2-7-93-12W4	Oil Sands 1	Micro-frac	156	3.2			20.5	Oil sand	Proskin et al., 1990b
2-7-93-12W4	Oil Sands 1	Micro-frac	170	4.7			27.6	Subcropping limestone	Proskin et al., 1990a
49.709°N, 112.935°W	Kipp Mine	Overcoring	180	3.3	4.2	5.0	18.3	All stresses measured	Kaiser et al., 1982
5-2-86-7W4	Oil Sands 3	Micro-frac	187	4.2			22.5	Shale	Proskin et al., 1990a
1-16-95-7W4	Oil Sands 2	Micro-frac	210	4.3			20.5	Oil sand	Proskin et al., 1990b
1-16-95-7W4	Oil Sands 2	Micro-frac	220	4.2 - 4.4			19.1 - 20.0	Oil sand	Proskin et al., 1990a
5-2-86-7W4	Oil Sands 3	Micro-frac	235	3.2 - 3.6			13.6 - 15.3	Oil sand	Proskin et al., 1990a
5-2-86-7W4	Oil Sands 3	Micro-frac	237	5.3			22.4	Subcropping limestone	Proskin et al., 1990b
55.982°N, 113.355°W	Wabasca	Micro-frac	240	6.4			26.7		Settari and Raisbeck, 1978
4-35-84-11W4	Athabasca	Micro-frac	291	4.6			15.8		Leshchyshyn and Seyer, 1990
56.370°N, 111.000°W	Gregoire Lake	Micro-frac	317	5.6			17.7		Holzhausen et al., 1980
54.643°N, 110.188°W	Cold Lake	Micro-frac Micro-frac Micro-frac	417 420 420	9.8 7.9 9.1			23.5 16.7 21.7		Settari and Raisbeck, 1978
54.590°N, 110.364°W	Cold Lake	Micro-frac	457	9.0			19.7		Imperial Oil, 1978
10-28-28-24W3	Kindersley	Micro-frac Micro-frac Micro-frac	680 705 729	14.7 9.4 16.0			21.6 13.3 21.9		Talebi et al., 1991
8-23-67-8W6	Wapiti	Micro-frac Micro-frac Micro-frac Micro-frac Micro-frac Micro-frac	1236 1242 1248 1254 1259.5 1264.5	30.1 31.0 32.1 34.0 30.3 32.3			24.1 25.1 25.8 27.2 24.1 25.6		McLellan, 1988a
C9-23-06-11W2	Midale	Micro-frac	1429-34	17.1-22.6			c.13.1	Horizontal well	McLellan et al., 1991
11-12-71-13W6	Elmworth	Micro-frac	2021-66	39.7-40.7		61.8-64.8	19.7	S_{Hmax} calculated	Wyman et al., 1980
3-8-12-12W2	Regina	Micro-frac	2065	35.7	51.6	40.7	17.3	S_{Hmax} S_V calculated	McLennan et al., 1986
c-16-I-93-P-1	Elmworth	Micro-frac Micro-frac Micro-frac Micro-frac Micro-frac	2073 2095 2128 2149 2165	40.7 34.5 38.6 42.3 39.0		63.0-71.0 51.0-57.0 61.0-63.0 65.0-72.0 62.0-65.0	19.6 16.5 18.1 19.7 18.0	S_{Hmax} calculated S_{Hmax} calculated S_{Hmax} calculated S_{Hmax} calculated S_{Hmax} calculated	Kry and Gronseth, 1982
3-8-12-12W2	Regina	Micro-frac Micro-frac	2168 2213	40.1 41.1	54.2 55.3	55.3 52.8	18.5 18.6	S_{Hmax} S_V calculated S_{Hmax} S_V calculated	McLennan et al., 1986
10-16-69-11W6	Elmworth	Micro-frac Micro-frac	2213 2241	30.0 36.0		40.0 51.0	13.6 16.1	S_{Hmax} calculated S_{Hmax} calculated	Kry and Gronseth, 1982
c-16-I-93-P-1	Elmworth	Micro-frac Micro-frac Micro-frac Micro-frac Micro-frac Micro-frac Micro-frac	2669 2679 2699 2717 2740 2750 2765	45.1 44.3 45.2 44.0 46.2 45.1 46.6		62.0-63.0 60.0-77.0 59.0-71.0 	16.9 16.5 16.7 16.2 16.9 16.4 16.9	S_{Hmax} calculated S_{Hmax} calculated S_{Hmax} calculated 	Kry and Gronseth, 1982
1-12-35-7W5	Caroline	Micro-frac Micro-frac	2992 2996	60.0 61.0			20.1 20.4		McLennan et al., 1982

has been "damaged" in the area adjacent to the wellbore. We have plotted depth-normalized reservoir pressures against depth-normalized fracture closure pressures and there is some degree of correlation, though not enough to clearly demonstrate that a reduction in reservoir pressure alone modifies mini-frac measurements of S_{Hmin}. Reduction in fluid pressures due to hydrocarbon production may be a factor, as was demonstrated by Salz (1977), but clearly there are other processes at work. The net result is that the closure stresses obtained from mini-fracs run in such sandstones tend to be lower than if the measurements had been made in the virgin reservoirs. This means that much of the mini-frac data will not be suitable for documenting natural stress magnitudes accurately, because the fracture closure pressures will underestimate S_{Hmin} in many cases.

The above comments are generalizations and they apply with varying degrees to the data plotted in Figure 29.5. Production history information, geomechanical aspects of any reservoir disruption and reservoir pressure would be required to assess individual closure stresses as measures of S_{Hmin}. What can be stated is that most of the shallower estimates of closure stress (above -1200 m) are likely to be close to virgin S_{Hmin} magnitudes, whereas most of the deeper ones are likely to underestimate S_{Hmin}.

Figure 29.6 plots formation leak-off test pressures that were measured in 35 wells at depths greater than -500 m. These are the pressures at which fluid begins to be lost to the formation when the drilling fluid pressure is raised by pumping to test the integrity of the strata below a string of cemented casing. Traditionally, this

Table 29.2 Formation leak-off and mini-frac closure pressures, Western Canada Sedimentary Basin.

Well identification	Type of measurement	Depth in metres below K.B.	Closure stress in MPa	Depth-normalized gradient of S_{Hmin} in kPa/m	Comments
12-30-11-1W5	Leak-off	735	18.4	25.0	? High tensile strength
13-14-33-10W4	Leak-off	1285	21.3	16.6	Max value for S_{Hmin}
06-33-34-28W4	Leak-off	2542	45.8	18.0	Max value for S_{Hmin}
11-27-35-5W5	Leak-off	3590	74.1	20.6	Max value for S_{Hmin}
07-33-36-10W5	Leak-off	3300	73.1	22.2	Max value for S_{Hmin}
12-10-38-7W5	Leak-off	2096	34.4	16.4	Max value for S_{Hmin}
16-19-38-7W5	Leak-off	2095	35.7	17.0	Max value for S_{Hmin}
11-03-39-11W5	Leak-off	751	19.3	25.7	? High tensile strength
14-24-40-25W4	Leak-off	1490	17.7	11.9	Max value for S_{Hmin}
11-27-42-16W5	Leak-off	3410	52.2	15.3	Max value for S_{Hmin}
16-10-47-1W5	Leak-off	2060	39.5	19.2	Max value for S_{Hmin}
08-14-47-13W5	Leak-off	3286	51.7	15.7	Max value for S_{Hmin}
03-27-47-16W5	Leak-off	3822	74.1	19.4	Max value for S_{Hmin}
05-13-48-13W5	Leak-off	2952	51.5	17.4	Max value for S_{Hmin}
12-13-48-13W5	Leak-off	3189	44.2	13.9	Max value for S_{Hmin}
11-09-48-12W5	Leak-off	3040	56.9	18.7	Max value for S_{Hmin}
06-22-54-21W5	Leak-off	3093	47.4	15.3	Max value for S_{Hmin}
12-07-55-19W5	Leak-off	2964	67.2	22.7	Max value for S_{Hmin}
07-05-58-6W6	Leak-off	1835	43.4	23.7	Max value for S_{Hmin}
06-12-62-25W4	Leak-off	970	10.8	11.1	? Injection pressure
07-25-62-6W6	Leak-off	605	8.7	14.4	Max value for S_{Hmin}
15-11-78-8W5	Leak-off	1704	26.7	15.7	Max value for S_{Hmin}
03-01-78-6W6	Leak-off	2330	30.8	13.2	Max value for S_{Hmin}
08-36-80-16W5	Leak-off	3510	39.9	11.4	? Injection pressure
10-16-88-3W5	Leak-off	573	15.5	27.0	? High tensile strength
09-36-89-9W6	Leak-off	1693	22.3	13.2	Max value for S_{Hmin}
05-17-90-24W5	Leak-off	1884	28.5	15.1	Max value for S_{Hmin}
14-27-91-7W5	Leak-off	768	12.0	15.6	Max value for S_{Hmin}
03-20-95-6W5	Leak-off	697	14.4	20.7	Max value for S_{Hmin}
01-03-96-6W5	Leak-off	688	16.4	23.8	Max value for S_{Hmin}
03-36-96-11W5	Leak-off	620	14.3	23.1	Max value for S_{Hmin}
10-29-96-11W6	Leak-off	500	13.6	27.2	? High tensile strength
13-20-97-10W5	Leak-off	501	10.9	21.8	Max value for S_{Hmin}
13-06-109-6W6	Leak-off	1741	19.1	11.0	? Injection pressure
14-27-117-3W6	Leak-off	1107	19.8	17.9	Max value for S_{Hmin}
08-17-36-6W5	Mini-frac	2741	36.4	13.3	
11-25-36-5W5	Mini-frac	2131	39.2	18.4	
03-05-38-8W5	Mini-frac	2922	41.4	14.2	
12-21-37-3W5	Mini-frac	2253	36.4	16.2	
14-08-39-3W5	Mini-frac	1510	22.1	14.6	
13-08-37-9W5	Mini-frac	3314	54.4	16.4	
06-14-38-9W5	Mini-frac	3005	52.2	17.4	
	Mini-frac	2454	41.7	17.0	
08-04-37-5W5	Mini-frac	2505	45.0	18.0	
09-24-41-25W4	Mini-frac	1545	21.3	13.8	
06-14-43-26W4	Mini-frac	1415	20.7	14.6	
08-15-45-4W5	Mini-frac	1238	20.2	16.3	Most of the closure stress magnitudes obtained from mini-frac pressure records are likely to under-estimate S_{Hmin} magnitudes, because the mini-fracs have frequently been run in reservoirs where the fluid pressure has been lowered through hydrocarbon production.
14-01-46-4W5	Mini-frac	1734	23.5	13.6	
06-11-46-28W4	Mini-frac	1618	19.3	11.9	
08-24-49-26W4	Mini-frac	1337	20.4	15.3	
04-02-50-6W5	Mini-frac	1581	22.5	14.2	
14-11-47-3W5	Mini-frac	1025	15.7	15.3	
15-12-48-9W5	Mini-frac	1620	24.5	15.1	
06-01-49-7W5	Mini-frac	1381	18.6	13.5	
16-03-48-2W5	Mini-frac	908	14.0	15.4	
08-31-49-6W5	Mini-frac	1257	19.0	15.1	
10-15-49-6W5	Mini-frac	1361	17.0	12.5	
06-29-49-6W5	Mini-frac	1329	20.0	15.0	
10-33-49-5W5	Mini-frac	1295	20.0	15.4	
04-05-50-6W5	Mini-frac	1327	18.0	13.6	
06-36-50-28W4	Mini-frac	1393	21.2	15.2	
08-09-51-27W4	Mini-frac	1300	18.2	14.0	
16-28-52-8W5	Mini-frac	1799	28.3	15.7	
13-31-46-15W5	Mini-frac	2001	25.8	12.9	
05-08-47-15W5	Mini-frac	2074	22.1	10.7	? Pore fluid pressure
14-32-46-16W5	Mini-frac	2197	38.0	17.3	
04-05-47-15W5	Mini-frac	1973	32.5	16.5	
05-20-47-14W5	Mini-frac	1979	23.0	11.6	
16-29-45-12W5	Mini-frac	2528	45.0	17.8	
11-12-49-18W5	Mini-frac	2433	41.5	17.1	
03-26-49-20W5	Mini-frac	2656	46.9	17.7	
02-23-51-13W5	Mini-frac	1820	28.9	15.9	

Well identification	Type of measurement	Depth in metres below K.B.	Closure stress in MPa	Depth-normalized gradient of S_{Hmin} in kPa/m	Comments
12-23-51-13W5	Mini-frac	1831	29.0	15.8	
06-16-05-14W4	Mini-frac	910	18.3	20.1	
05-28-05-5W4	Mini-frac	1100	9.0	8.2	? Pore fluid pressure
05-31-11-18W4	Mini-frac	1346	18.4	13.7	
11-08-30-10W5	Mini-frac	4500	81.6	18.1	
08-29-36-13W5	Mini-frac	2768	65.1	20.3	
08-10-24-12W4	Mini-frac	937	12.4	13.2	
06-20-24-12W4	Mini-frac	1018	19.0	18.7	
12-30-24-12W4	Mini-frac	1004	12.7	12.6	
06-05-30-4W5	Mini-frac	2357	34.9	14.8	
08-30-34-6W4	Mini-frac	950	16.0	16.8	
11-05-39-3W4	Mini-frac	778	10.7	13.8	
02-21-38-4W5	Mini-frac	2270	32.5	14.3	
08-28-38-3W5	Mini-frac	2196	34.0	15.5	
06-17-39-2W5	Mini-frac	1911	28.6	15.0	
16-17-39-2W5	Mini-frac	1905	30.1	15.8	
08-27-34-7W5	Mini-frac	2762	44.0	15.9	
08-09-35-7W5	Mini-frac	2875	46.0	16.0	
06-20-33-5W5	Mini-frac	2578	49.0	19.0	
14-09-33-5W5	Mini-frac	2588	49.2	19.0	
16-03-34-8W5	Mini-frac	2492	33.9	13.6	
01-10-34-8W5	Mini-frac	2468	40.5	16.4	
08-02-34-8W5	Mini-frac	2357	26.5	11.2	? Pore fluid pressure
04-15-34-8W5	Mini-frac	2641	64.1	24.3	
02-26-36-9W5	Mini-frac	2891	38.0	13.2	
12-18-36-8W5	Mini-frac	2742	38.2	13.9	
01-01-36-9W5	Mini-frac	2730	50.0	18.3	
08-16-35-3W5	Mini-frac	2107	28.6	13.6	
14-17-35-3W5	Mini-frac	2101	27.6	13.1	
06-35-36-5W5	Mini-frac	2463	42.2	17.1	
16-17-36-5W5	Mini-frac	2689	41.5	15.4	
14-01-37-5W5	Mini-frac	2398	39.0	16.3	
	Mini-frac	2097	34.0	16.2	
06-23-36-5W5	Mini-frac	2510	40.3	16.1	
11-22-55-19W5	Mini-frac	1971	37.8	19.2	
07-36-61-4W6	Mini-frac	1893	43.1	22.8	
16-09-62-4W6	Mini-frac	1838	33.5	18.2	
04-31-66-7W6	Mini-frac	1323	28.2	21.3	
10-34-62-26W5	Mini-frac	1845	29.0	15.7	
06-01-63-26W5	Mini-frac	1850	26.3	14.2	
08-06-63-26W5	Mini-frac	1964	28.0	14.3	
03-16-63-8W6	Mini-frac	3066	58.2	19.0	
04-29-63-19W5	Mini-frac	1815	27.8	15.3	
06-07-67-7W6	Mini-frac	1329	26.8	20.2	
13-07-67-7W6	Mini-frac	1278	25.8	20.2	
11-20-68-9W6	Mini-frac	2147	31.0	14.4	
08-13-72-8W5	Mini-frac	2085	34.2	16.4	
02-10-71-4W5	Mini-frac	1769	26.2	14.8	
12-30-71-3W5	Mini-frac	1663	27.0	16.2	
10-26-71-5W5	Mini-frac	1844	27.0	14.6	
08-13-72-8W5	Mini-frac	1686	26.0	15.4	
05-23-72-5W5	Mini-frac	1675	28.7	17.1	
10-23-72-4W5	Mini-frac	1612	23.0	14.3	
02-07-73-4W5	Mini-frac	1621	27.0	16.7	
08-12-73-5W5	Mini-frac	1635	24.0	14.7	
12-16-73-4W5	Mini-frac	1614	26.5	16.4	
02-17-78-3W5	Mini-frac	1725	28.0	16.2	
08-25-77-10W6	Mini-frac	1870	31.7	17.0	
12-20-79-7W5	Mini-frac	1702	31.5	18.5	
04-18-79-7W5	Mini-frac	1706	30.2	17.7	
11-26-78-11W6	Mini-frac	1855	34.2	18.4	
10-22-84-18W6	Mini-frac	973	19.5	20.0	
05-26-84-18W6	Mini-frac	946	21.1	22.3	
08-4-110-8W6	Mini-frac	1905	36.0	18.9	
08-36-29-11W5	Mini-frac	4714	100.5	21.3	
05-15-06-10W2	Mini-frac	1394	16.5	11.8	
11-20-06-10W2	Mini-frac	1388	17.0	12.2	
14-13-09-28W1	Mini-frac	728	12.6	17.3	
d-1-D-94-P-70	Mini-frac	613	13.8	22.5	
d-75-D-94-P-7	Mini-frac	639	9.5	14.9	
06-04-02-29W1	Mini-frac	1029	15.4	15.0	

Figure 29.3 Locations of stress magnitude measurements made by overcoring and micro-frac testing in the Western Canada Sedimentary Basin. The measurements are listed in Table 29.1 and plotted against depth in Figure 29.4.

pressure is interpreted as recording fracture initiation, or injectivity, into the rocks that surround the borehole at the top of the open interval, below the lowest casing shoe. The 35 formation leak-off test records were checked for interpretational accuracy in this study and, as can be seen, there is a considerable scatter to the pressures (Fig. 29.6). The values below a gradient of 12 kPa/m, close to hydrostatic pressure levels (c. 10 kPa/m), possibly simply record the injection of drilling mud into permeable rocks without any induced fracturing occurring. Hence, they are likely to be indicative of fluid injectivity, not in-situ stresses, and should be ignored. Values near 24 kPa/m are close to the typical overburden stress levels (S_V) for depths greater than 1200 m. Possibly, such rocks resisted easy fracturing because their tensile strengths were high. It is suspected that what has been measured in these anomalous cases are "formation breakdown" pressures that are likely to be significantly larger than the closure stresses (S_{Hmin}) for the fractures, hence they too should be ignored. The median population (14 kPa/m - 24 kPa/m) are likely to record fracture initiation in rocks with low tensile strengths and, therefore, these leak-off pressures will overestimate S_{Hmin} by a small amount. They can be used to place an upper limit on S_{Hmin} magnitudes (Breckels and Van Eekelen, 1981; Ervine and Bell, 1987; Bell, 1990).

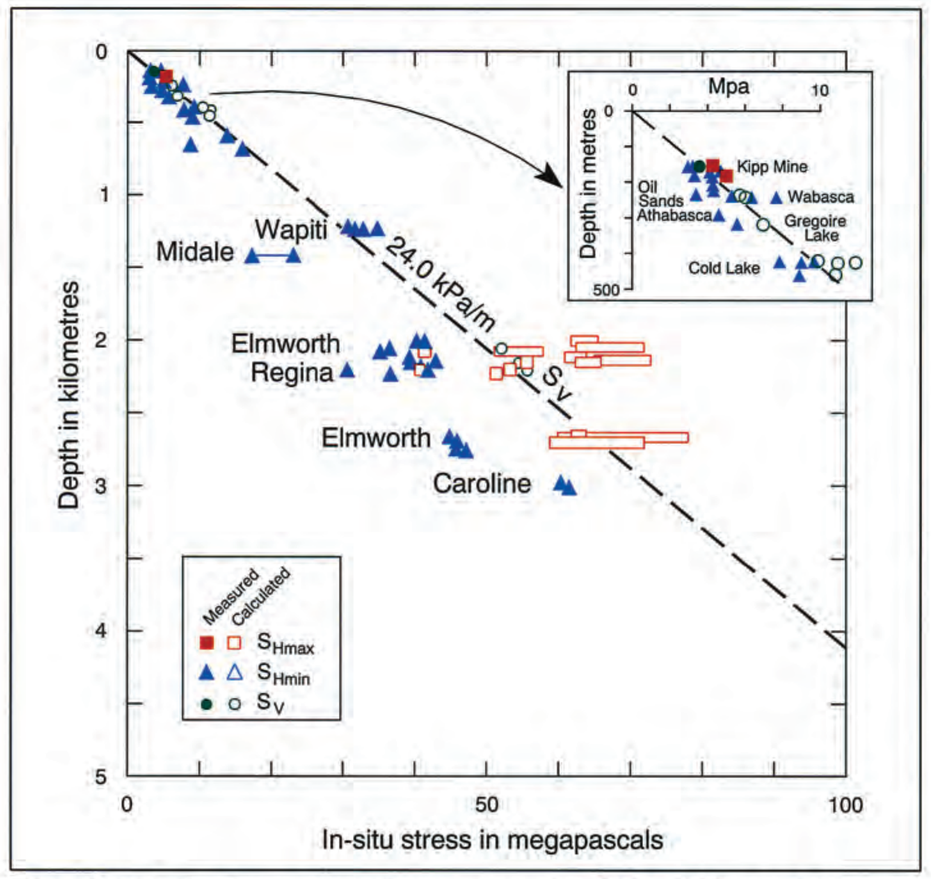

Figure 29.4 In-situ stress magnitude measurements of high reliability made by overcoring and by micro-fracing in the Western Canada Sedimentary Basin. All three principal stresses can be quantified separately by overcoring, but only S_{Hmin} can be measured independently during micro-fracing. S_V and S_{Hmax} are estimated as discussed in the text. Locations are shown in Figure 29.3 and details of the stress measurements are listed in Table 29.1.

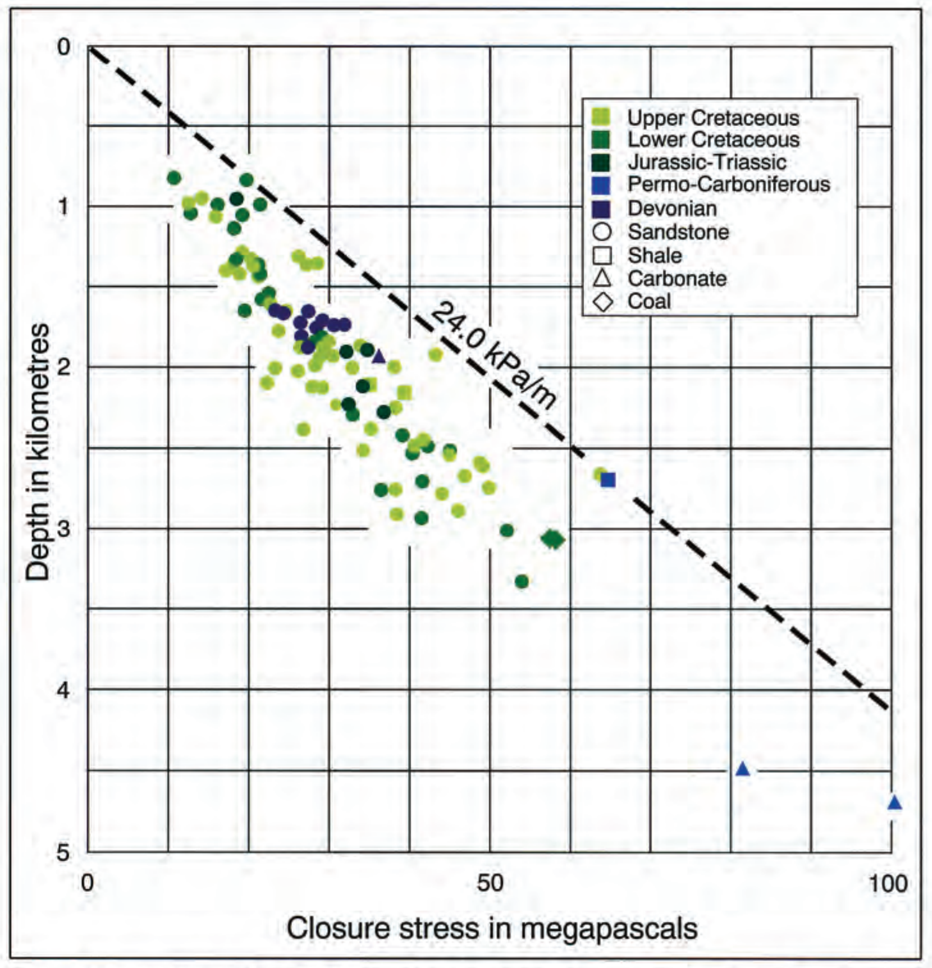

Figure 29.5 Closure stresses derived from mini-frac treatments in Alberta wells. Most of the measurements underestimate S_{Hmin} because prior production of hydrocarbons has led to local reductions in in-situ stress magnitudes. Original data are listed in Woodland and Bell (1989), and are summarized in Table 29.2.

Implications of Stress Magnitudes in Western Canada

A number of shallow-depth micro-frac measurements of S_{Hmin} have been made in the oil sands and heavy oil deposits of northeastern Alberta (Table 29.1, Figs. 29.3, 29.4). Some of the results suggest that the vertical stress may be the smallest principal stress at depths of less than 500 to 600 m (e.g., Settari and Raisbeck, 1978), while others imply that the vertical stress and the smaller horizontal principal stress are of closely similar magnitudes (e.g., Proskin et al., 1990a,b). It is not clear how representative these shallow measurements are for the rest of the basin. The few reliable deep measurements from micro-fracturing (Fig. 29.4) are all from the western flank of the basin (Fig. 29.3). They point to a stress regime with $S_{Hmax} > S_V > S_{Hmin}$ in the Elmworth area (Kry and Gronseth, 1983), in the Caroline area (McLennan et al., 1982), and possibly around the Kidd Mine (Kaiser et al., 1982), where overcoring measurements support this relationship. On the other hand, a thrust regime, with $S_{Hmax} > S_{Hmin} > S_V$, may possibly exist in the Wapiti area (McLellan, 1988a). In Saskatchewan (McLennan et al., 1986, McLellan et al., 1992), S_V may be the largest principal stress. In other parts of the basin, the stress magnitude indicators are not accurate enough to unequivocally identify the regime.

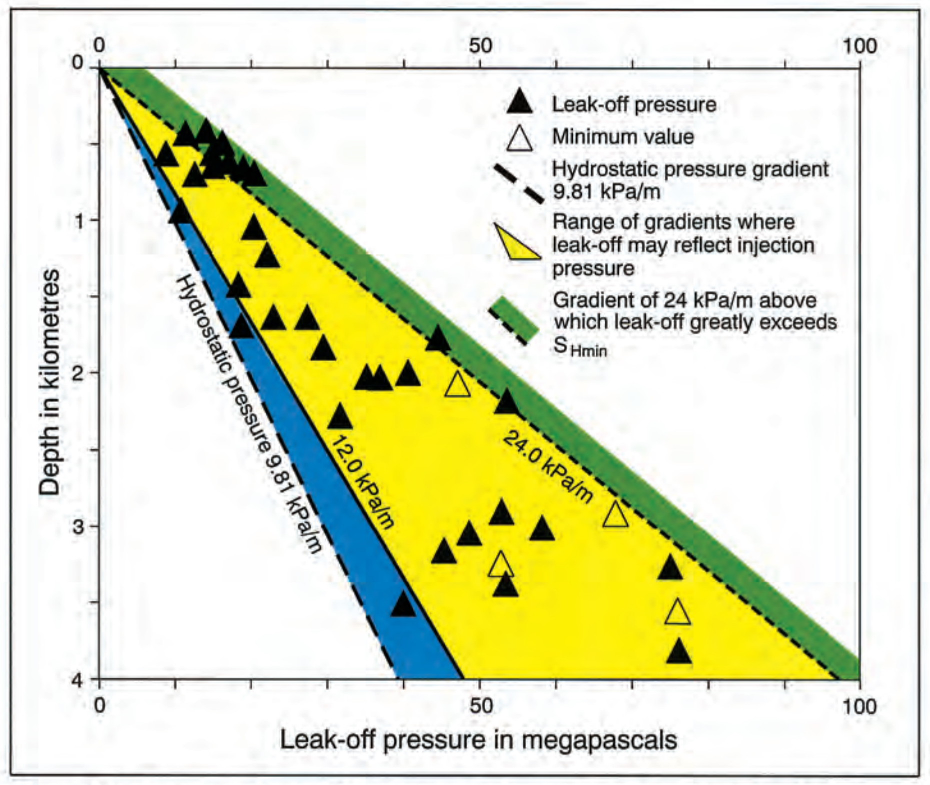

Figure 29.6 Formation leak-off test pressures from 35 wells in Alberta in which the tests were performed at depths greater than 500 m. Pressure measurements with gradients less than 12 kPa/m possibly represent fluid injection pressures with no fracturing. Tests with gradients greater than 24 kPa/m may record fractures initiated in rocks with high tensile strengths. The values between 14 and 24 kPa/m are likely to be closer to S_{Hmin} and can be used as upper limits for its magnitude. Well locations and test details are given in Table 29.2.

In earlier interpretations (Woodland and Bell, 1989; Bell and Price, 1989; Bell and McCallum, 1990), it was suggested that the mini-frac closure pressures yielded magnitudes of S_{Hmin} that were precise enough to use for identifying the relative magnitudes of the principal stresses at the site. With this reasoning, Woodland and Bell (1989) concluded that much of the central part of the Western Canada Sedimentary Basin lay within a normal fault regime, where $S_V > S_{Hmax} > S_{Hmin}$ was widely present. Later, Bell and Price (1989) and Bell and McCallum (1990) suggested that mini-frac closure stresses could also be used to map lateral variations of S_{Hmin} across the basin, and drew conclusions from the apparent configurations. These procedures can no longer be considered valid in light of the apparent inaccuracies in the closure stress magnitudes that have been measured in productive sandstone reservoirs, as discussed above.

To obtain a reliable three-dimensional picture of stress magnitudes in the Western Canada Sedimentary Basin we need more data. Until these become available, we shall not have a clear idea of relative and absolute magnitudes of principal stresses in most parts of the basin, nor will we be able to speculate on the evolution of its stress regime, or on the implications of any regional variations in stress magnitudes. Today's data give an idea of expected S_{Hmin} magnitudes locally, but little more.

Stress Orientation Measurements

In the Western Canada Sedimentary Basin, the axes of the present-day horizontal principal stresses recorded in publications are indicated by breakouts (181 wells), hydraulic fracture orientation (1 well), anelastic strain recovery (2 wells), differential strain curve analysis (1 well), waterflood breakthrough (2 locations), overcoring measurements (3 sites), near-surface stress release features (2 sites) and microseismic monitoring (1 site).

Breakouts

Breakouts are spalled cavities that occur on opposite sides of a borehole wall. They form because the well, being a cylindrical opening in rock, distorts and locally amplifies the far-field stresses, so as to produce caving in the borehole wall (Bell and Gough, 1979). If the horizontal principal stresses are of unequal magnitude, the wall rock is squeezed anisotropically, and caving occurs preferentially on opposite sides of the hole, perpendicular to the trajectory of S_{Hmax} (Fig. 29.7). Thus, breakouts that occur in a near-vertical well can usually be used to diagnose stress anisotropy and also to map the orientations of the horizontal principal stresses.

Breakouts have been previously identified and oriented by studying 4-arm dipmeter logs from 181 wells in the Western Canada Sedimentary Basin (Table 29.3). The total thicknesses of all breakout intervals in a single well ranged from 2 m to 2087 m. The shallowest breakout occurred at a depth of 113 m; the deepest at 5485 m. The majority reported here were identified between depths of 1000 and 3500 m. The largest number of breakout intervals measured in a single well was 84; the smallest was 1. Of the 181 wells examined, 144 contain only a single major population of breakout orientations. Thirty seven wells have secondary minor populations, commonly with mean azimuths at approximately 90° to the major breakout population. Consistency in breakout orientation with depth is widely observed, no matter what type or age of rock is involved.

Breakout orientations have been mapped for Paleozoic and Mesozoic rocks (Figs. 29.8 ,29.9) and both data sets have been combined for the horizontal stress trajectory map (Fig. 29.10). This map has been constructed chiefly from the mean breakout orientations in 181 wells (Table 29.3), but it honours the horizontal principal stress orientations yielded by the other measurements (Table 29.4). The reliance on breakouts is justified because these features have

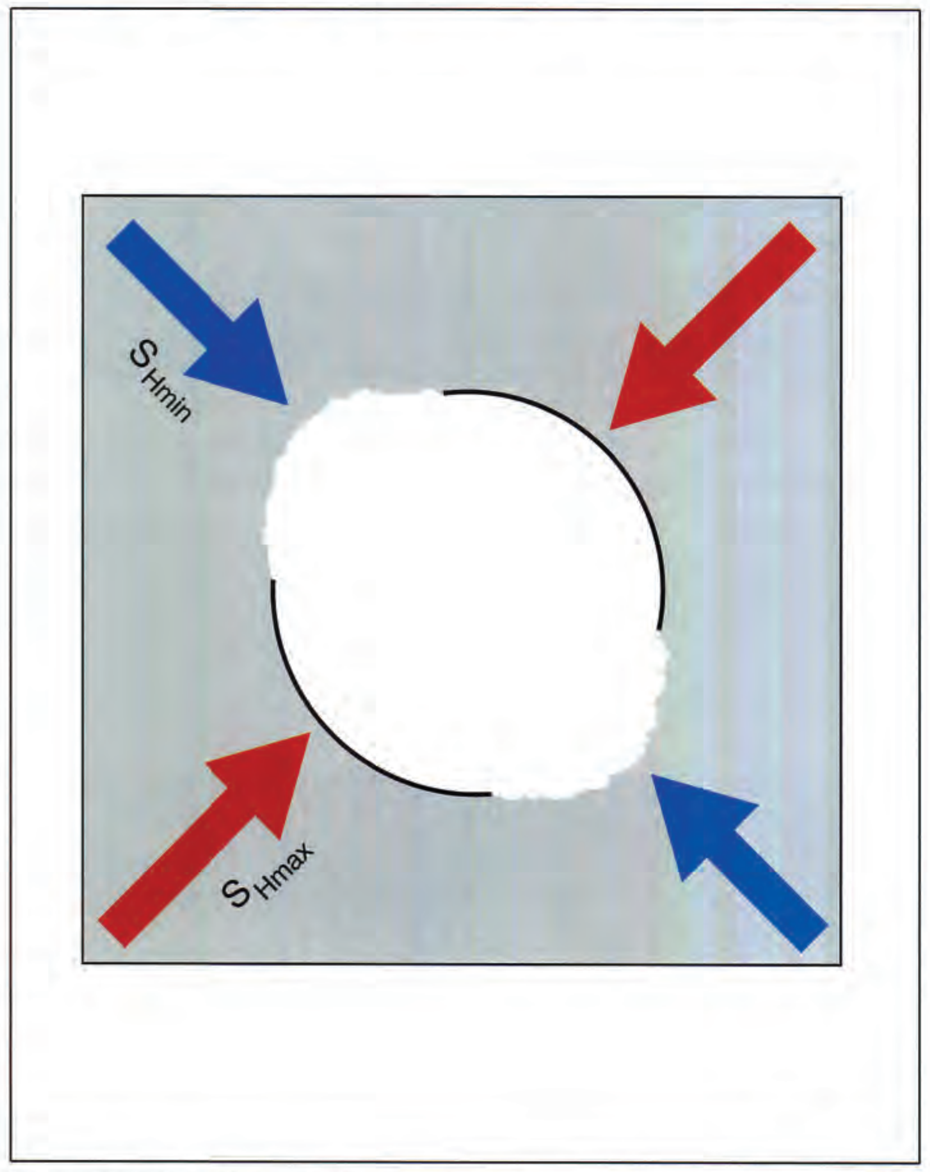

Figure 29.7 Vertical view of a borehole breakout in a vertical well. The long axis of elliptical caving is perpendicular to S_{Hmax}, the larger horizontal stress.

Table 29.3 Mean breakout azimuths in degrees for 181 wells in the Western Canada Sedimentary Basin.

Well name	Location	ALL Pop 1	ALL Pop 2	MESO Pop 1	MESO Pop 2	PALZ Pop 1	PALZ Pop 2
03-02-02-26W4	49.089N, 113.381W	142.8		143.0		141.0	
06-28-04-27W3	49.326N, 109.582W	139.5		139.5			
16-33-04-9W2	49.348N, 103.151W	100.1				100.1	
01-04-05-9W2	49.351N, 101.151W	36.2	153.9			36.2	153.9
11-05-05-27W3	49.359N, 109.605W	132.8		132.8			
09-13-05-13W2	49.388N, 103.622W	37.4	164.1			37.4	164.1
13-15-05-25W2	49.391N, 105.298W	136.5		136.5			
C3-05-06-10W2	49.442N, 103.327W	121.0				121.0	
16-22-06-3W2	49.493N, 102.321W	95.7		95.7			
06-11-09-4W5	49.719N, 114.445W	127.2	57.2	63.0	166.0	116.1	66.8
16-07-09-18W3	49.726N, 108.422W	102.7		102.7			
04-23-09-4W5	49.745N, 114.451W	121.4				121.4	
10-11-10-17W4	49.810N, 112.204W	154.5		154.5			
13-25-10-16W4	49.857N, 112.057W	158.4		158.4			
08-02-11-16W4	49.879N, 112.078W	145.5		145.5			
09-01-12-29W4	49.970N, 113.830W	146.6		146.6			
11-19-12-25W4	50.014N, 113.409W	129.1		129.1			
10-25-12-26W4	50.028N, 113.426W	131.0				131.0	
10-30-12-21W4	50.028N, 112.857W	151.2		151.2			
14-30-12-21W4	50.032N, 112.863W	136.0		136.0			
14-36-12-18W4	50.047N, 112.339W	167.3		167.3			
10-16-13-26W4	50.087N, 133.494W	135.6		136.0		135.0	
10-04-15-3W5	50.232N, 114.354W	141.9		141.9			
10-21-15-15W4	50.276N, 112.007W	162.5		162.5			
10-16-16-3W5	50.349N, 114.354W	139.6		139.6			
07-35-18-21W4	50.563N, 112.786W	180.7		170.0		184.0	
06-11-19-3W4	50.593N, 110.319W	152.8	80.0	152.8	80.0		
11-12-19-2W5	50.596N, 114.155W	136.7		135.7		139.6	
05-27-20-4W5	50.593N, 114.484W	153.4	74.0	153.4	74.0		
06-07-21-4W5	50.767N, 114.547W	149.1		149.1			
16-10-21-3W4	50.774N, 110.331W	165.6		165.6			
10-29-21-19W5	50.815N, 112.599W	147.0		147.0			
05-15-22-5W5	50.869N, 114.622W	134.1		134.1			
15-15-24-6W5	51.051N, 114.755W	126.3	46.5	126.3	46.5		
12-33-25-6W5	51.178N, 114.790W	154.9		154.9			
06-33-28-5W5	51.437N, 114.649W	145.1		145.1			
10-21-29-5W5	51.499N, 114.644W	144.9				144.9	
12-02-30-5W5	51.542N, 114.608W	145.3				145.3	
06-16-33-5W5	51.830N, 114.938W	157.4		157.4			
07-17-33-7W5	51.830N, 114.956W	136.3		136.3			
07-22-33-8W5	51.844N, 115.050W	151.5	61.0	151.5	61.0		
A02-13-34-11W5	51.914N, 115.428W	138.3				138.3	
03-32-34-8W5	51.957N, 115.103W	139.3		139.3			
07-03-35-8W5	51.975N, 115.058W	139.7	40.3	139.7	40.3		
05-05-35-11W5	51.975N, 115.546W	169.8	28.5			169.8	28.5
09-06-35-26W3	51.979N, 109.695W	142.5				142.5	
01-12-35-7W5	51.986N, 114.862W	148.7		148.7			
11-20-35-1W5	52.023N, 114.112W	132.4				132.4	
8-11-36-21W4	52.077N, 112.888W	153.1	48.8	152.0	48.8	156.2	
06-08-36-8W5	52.077N, 115.112W	122.7		122.7			
02-16-36-28W3	52.088N, 109.939W	150.5		150.5			
11-13-36-7W5	52.095N, 114.874W	153.1				153.1	
06-17-37-9W5	52.179N, 115.255W	121.9		121.9			
14-21-37-11W5	52.201N, 115.516W	151.0		151.5		146.8	
06-01-38-10W5	52.237N, 115.302W	142.9				142.9	
07-10-38-2W5	52.252N, 114.201W	142.0		142.0			
10-23-38-3W5	52.285N, 114.320W	141.6				141.6	
11-36-38-27W3	52.314N, 109.731W	143.7		143.7			
04-04-39-11W5	52.321N, 115.534W	144.4				144.4	
12-05-39-26W3	52.328N, 109.718W	136.8		136.8			
16-24-39-21W4	52.376N, 112.887W	141.8		143.0		141.6	

Pop - Population, MESO - Mesozoic, PALZ - Paleozoic.

Well name	Location	ALL Pop 1	ALL Pop 2	MESO Pop 1	MESO Pop 2	PALZ Pop 1	PALZ Pop 2
10-35-39-2W5	52.401N, 114.179W	130.2		130.2			
15-10-40-13W4	52.434N, 111.789W	130.9		130.9			
07-25-40-12W5	52.470N, 115.594W	130.9				130.9	
06-25-40-14W5	52.470N, 115.888W	149.7	44.2	149.2	44.2	173.3	
16-10-41-12W4	52.521N, 111.639W	143.3		143.3			
09-29-42-25W3	52.648N, 109.556W	117.7		117.7			
06-07-43-24W3	52.688N, 109.476W	162.9		162.9			
11-22-43-13W5	52.721N, 115.807W	144.6				144.6	
14-10-44-22W4	52.783N, 113.115W	133.7		133.0		135.0	
11-21-44-20W5	52.808N, 116.846W	134.4	29.0	134.4	29.0		
10-24-45-24W4	52.896N, 113.351W	150.5		150.5			
10-25-45-15W5	52.910N, 116.042W	148.3		153.1		147.8	
10-27-45-16W5	52.910N, 116.236W	135.3				135.3	
06-30-46-17W5	52.994N, 116.459W	143.1	38.4	143.1	38.4		
11-27-46-21W4	52.998N, 112.970W	138.5		139.4		130.0	
16-25-47-21W5	53.089N, 116.930W	148.1				148.1	
03-32-47-13W5	53.092N, 115.870W	131.3				131.3	
06-30-48-12W5	53.169N, 115.748W	140.4				140.4	
15-28-48-13W5	53.176N, 115.840W	137.7				137.7	
10-32-48-4W5	53.187N, 114.547W	120.0		120.0			
13-05-49-10W5	53.205N, 115.437W	136.9				136.9	
07-09-49-24W5	53.212N, 117.448W	150.8	60.7	150.8	60.7		
15-15-49-11W5	53.234N, 115.523W	138.1				138.1	
06-36-49-23W5	53.267N, 117.235W	137.1	12.5			137.1	12.5
03-36-49-23W5	53.276N, 117.235W	149.4	83.3	149.4	83.3		
			16.3		16.3		
01-09-50-12W5	53.296N, 115.687W	137.7				137.7	
06-12-50-11W5	53.300N, 115.480W	126.3				126.3	
10-12-50-27W5	53.303N, 117.814W	29.0	148.0	38.7	153.7	16.6	
02-14-50-22W5	53.311N, 117.107W	138.7		133.9		140.9	
06-20-50-15W5	53.329N, 116.162W	132.5		143.0		132.5	
14-22-50-11W4	53.332N, 111.532W	146.4		146.4			
14-20-50-12W5	53.336N, 115.724W	122.4		124.1		119.2	
10-04-51-9W5	53.376N, 115.265W	131.5				131.5	
08-08-51-9W5	53.387N, 115.283W	134.7		134.7			
05-09-51-9W5	53.387N, 115.277W	147.8				147.8	
04-26-51-11W5	53.427N, 115.523W	119.8				119.8	
06-30-51-20W5	53.431N, 116.942W	129.4				129.4	
03-05-52-21W5	53.456N, 117.065W	142.1				142.1	
06-01-52-13W5	53.460N, 115.790W	131.8				131.8	
2D1-10-52-23W3	53.471N, 109.305W	120.7		120.7			
07-10-52-10W5	53.474N, 115.388W	132.2				132.2	
13-09-52-8W5	53.481N, 115.129W	137.4	80.0	142.4	80.0	127.4	
16-16-52-21W5	53.496N, 117.028W	124.9				124.9	
12-19-53-8W5	53.594N, 115.179W	120.5				120.5	
11-23-53-2W6	53.594N, 118.187W	151.5		151.5			
01-16-55-27W5	53.747N, 117.946W	132.9		136.3		129.8	
11-28-55-6W4	53.783N, 110.838W	146.3		146.3			
11-24-56-14W5	53.856N, 115.950W	136.2				136.2	
04-29-57-3W5	53.951N, 114.420W	133.8				133.8	
14-09-58-24W4	54.005N, 113.515W	148.3				148.3	
12-23-58-18W5	54.031N, 116.576W	137.9				137.9	
01-26-58-18W5	54.038N, 116.558W	135.5				135.5	
02-01-59-18W5	54.067N, 116.561W	133.6				133.6	
06-06-59-17W5	54.071N, 116.542W	138.7				138.7	
12-13-59-18W5	54.104N, 116.573W	136.5				136.5	
05-22-59-4W4	54.114N, 110.526W	132.0		132.0			
02-29-59-22W5	54.125N, 117.260W	137.6	70.7	137.1	75.7	137.8	68.4
10-07-60-14W5	54.176N, 116.086W	151.3	24.5			151.3	24.5
16-23-62-20W5	54.383N, 116.879W	147.1		147.1			
07-04-63-26W4	54.420N, 111.161W	123.7				123.7	

Pop - Population, MESO - Mesozoic, PALZ - Paleozoic.

Well name	Location	ALL Pop 1	ALL Pop 2	MESO Pop 1	MESO Pop 2	PALZ Pop 1	PALZ Pop 2
06-13-63-8W4	54.449N, 111.079W	141.8		141.8			
06-27-65-5W4	54.653N, 110.676W	144.8		144.8			
12-08-66-5W4	54.700N, 110.732W	131.0		131.0			
10-26-66-5W6	54.744N, 118.639W	130.5		130.5			
2b-11-67-8W6	54.779N, 119.103W	134.0		134.0			
2b-14-67-8W6	54.797N, 119.097W	131.0		131.0			
13-20-67-9W5	54.820N, 115.346W	127.9				127.9	
10-16-69-11W6	54.976N, 119.611W	120.5		120.5			
13-19-69-8W6	54.994N, 119.217W	131.3				131.3	
10-11-71-11W6	55.136N, 119.574W	133.8		133.8			
10A-03-73-23W6	55.296N, 110.835W	131.1		131.1			
11-01-76-2W6	55.558N, 118.171W	112.2	86.7			112.2	86.7
14-35-79-23W6	55.896N, 121.488W	120.9	83.7	120.9	83.7		
13-26-80-22W4	55.969N, 113.343W	139.5		139.5			
05-03-81-9W5	55.991N, 115.330W	96.0	108.7			96.0	108.7
10-09-81-9W5	56.009N, 115.343W	123.4				123.4	
04-15-81-9W5	56.016N, 115.330W	116.6				116.6	
02-20-81-9W5	56.031N, 115.369W	115.6				115.6	
04-20-81-9W5	56.031N, 115.382W	124.7	49.4	121.1	15.5	129.5	66.4
14-21-81-9W5	56.042N, 115.350W	120.9				120.9	
11-36-81-10W5	56.067N, 115.428W	109.3				109.3	
09-05-82-9W5	56.082N, 115.363W	67.1				67.1	
12-24-82-6W6	56.125N, 118.806W	105.8				105.8	
16-24-82-12W6	56.129N, 119.726W	117.2		117.2			
11-29-82-5W6	56.140N, 118.747W	105.9				105.9	
09-18-83-6W6	56.198N, 118.925W	115.4				115.4	
07-24-83-7W4	56.209N, 110.963W	123.5		129.0		118.0	
10-23-83-7W4	56.213N, 110.989W	150.0	49.2	150.0	49.2		
07-07-86-1W6	56.442N, 118.142W	114.3				114.3	
04-30-87-8W5	56.569N, 115.275W	118.1	57.0			118.1	57.0
10-29-87-8W5	56.576N, 115.235W	115.5				115.5	
06-29-88-7W5	56.660N, 115.082W	133.9				133.9	
d-53-B-94-A-13	56.798N, 121.653W	125.8		125.8			
01-28-96-5W6	57.354N, 118.735W	148.5				148.5	
10-25-96-10W6	57.362N, 119.473W	136.6				136.6	
11-01-100-20W5	57.652N, 117.137W	154.5	53.6			154.5	53.6
b-14-G-94-J-2	58.094N, 122.672W	152.3				152.3	
d-84-G-94-J-8	58.406N, 122.166W	157.0				157.0	
07-18-109-7W6	58.463N, 119.154W	13.0				13.0	
15-29-109-8W6	58.499N, 119.293W	141.8				141.8	
05-33-109-8W6	58.506N, 119.279W	115.2				115.2	
10-17-110-9W6	58.554N, 119.461W	53.2	164.0			53.2	164.0
d-35-J-94-I-12	58.698N, 121.678W	153.6				153.6	
09-09-112-7W6	58.714N, 119.102W	160.7				160.7	
03-21-112-6W6	58.735N, 118.947W	159.0				159.0	
13-35-112-10W6	58.775N, 119.574W	153.5	85.0			153.5	85.0
12-33-114-5W6	58.946N, 118.785W	119.8				119.8	
05-28-115-4W6	59.015N, 118.622W	153.3				153.3	
15-29-115-3W6	59.023N, 118.466W	145.9	188.3			145.9	188.3
03-01-116-1W6	59.041N, 118.017W	146.4	65.3			146.4	65.3
15-09-116-6W6	59.066N, 118.950W	172.2	86.2			172.2	86.2
12-33-116-6W6	59.121N, 118.964W	139.6	48.7			139.6	48.7
14-36-116-6W6	59.124N, 118.871W	43.2				43.2	
14-09-118-8W6	59.241N, 119.298W	141.3		128.6		159.8	
09-15-118-8W6	59.252N, 119.255W	128.7				128.7	
02-36-118-8W6	59.288N, 119.206W	153.0	60.1			153.0	60.1
03-01-119-9W6	59.303N, 119.398W	140.4	54.7			140.4	54.7
03-11-121-7W6	59.491N, 119.081W	159.2				159.2	
b-42-I-94-P-11	59.702N, 121.059W	172.3	77.5			172.3	77.5
b-45-A-94-P-14	59.785N, 121.059W	149.0	63.1			149.0	63.1

Pop - Population, MESO - Mesozoic, PALZ - Paleozoic.

proved to be extraordinarily sensitive orientation indicators of contemporary stress. Table 29.3 lists the mean azimuths for all the breakout populations identified in the 181 wells and also separates the mean breakout directions observed in Paleozoic rocks (Fig. 29.8) and in Mesozoic rocks (Fig. 29.9).

Other Orientation Indicators

The horizontal stress orientations documented by mean azimuths of breakouts in wells are supported by measurements made using other techniques (Table 29.4).

Bell (1985) reported updip bed slip in Mississippian limestones in roadcuts near Exshaw, Alberta and in the nearby Kananaskis Valley. This phenomenon was interpreted as near-surface stress release and suggested S_{Hmax} azimuths of 049° and 032° at the two respective localities. In the same area, two overcored boreholes in Mesozoic rocks in the roof of the Wilson Mine at Canmore gave S_{Hmax} azimuths between 055° and 066° (Grant, 1970). Other overcoring measurements in Cretaceous rocks at the Kipp Mine in southern Alberta suggested S_{Hmax} orientations of 070° and 090° (Kaiser et al., 1982). Three hundred and seven overcoring stress measurements were made in seven test holes drilled into Lower Cretaceous sediments at the W.A.C. Bennett dam site in northeastern British Columbia. Based on the results of these measurements, Imrie (1991) interpreted an S_{Hmax} orientation of 076° for the central and southeastern area beneath the powerhouse and a 020° orientation for the northwestern area. The latter measurements were made within 200 m of the Peace River canyon wall, which is also aligned at approximately 020°, so they may not be representative of the regional stress signature. Other overcoring stress measurements have been made farther downstream at Dam Site C in northeastern British Columbia, in Lower Cretaceous sediments a few hundred metres from the banks of the Peace River. They yield east-west axes for S_{Hmax} but, since this orientation closely parallels the river banks and may not be regionally representative, it is not plotted on Figure 29.9.

Imperial Oil (1978) reported 045°-trending vertical hydraulic fractures in Cretaceous rocks at Cold Lake, based on heavy oil production research. McLennan et al. (1986) interpreted oriented packer impressions of induced fractures in lower Paleozoic rocks at the University of Regina well site and reported S_{Hmax} azimuths of 070° and 071°. Waterflood breakthrough in Cretaceous Cardium sandstone reservoirs at Pembina is attributed to inadvertent hydraulic fracturing. McLeod (1977) and Hassan (1982) reported connections between NE-SW-aligned wells, suggesting an approximate 045° orientation for S_{Hmax}. In a multi-facetted study of Cretaceous Cardium sandstones at Wapiti in Alberta (McLellan, 1988a), anelastic strain recovery measurements made on newly cored samples suggested that S_{Hmax} was oriented at 036°. Subsequent differential strain curve analysis of the same cores gave an S_{Hmax} azimuth of 043°. Fractures were propagated from the same well in which these cores were taken and monitored seismically. The results suggested that the induced fractures propagated along a direction of 035° (+/-15°). At Kindersley, in Saskatchewan, seismic monitoring suggested that an induced fracture in the Cretaceous Viking Formation propagated along an S_{Hmax} azimuth of 052° (Talebi et al., 1991). Anelastic strain recovery was also monitored on horizontal core samples of Mississippian carbonates recovered from a well at Midale in Saskatchewan and the measurements suggested that S_{Hmax} was oriented between 055° and 070°.

These stress directions, which have been obtained independently of breakouts, are also shown on the maps portraying the mean breakout azimuths for Paleozoic and Mesozoic rocks (Figs. 29.8, 29.9). On these maps, they are oriented to show S_{Hmin} directions.

Implications of Stress Orientations in Western Canada

On a local scale, the stress trajectories are useful for predicting the orientations of hydraulic fractures (Hubbert and Willis, 1957; Hassan, 1982).Typically, below depths of about 500 m, fractures will be vertical and will trend parallel to S_{Hmax} trajectories. Such information is helpful for planning secondary recovery programs that involve hydraulic fractures, for directed fracture operations, and for effectively directing inclined and horizontal wells (Bell and Babcock, 1986; McLellan et al., 1992).

With the recent surge in horizontal drilling of fractured reservoirs, there has been much interest in determining whether fractures trending in certain directions are more likely to remain open and productive compared to fractures trending in other directions. This information has a direct bearing on how the horizontal wells are drilled. Stress information can help predict which of several fracture sets is likely to contribute most to long-term hydrocarbon production. As yet, there are very few published case histories that demonstrate the significance of the in-situ stress orientations in fractured reservoirs. However, all other factors being equal, fractures running NE-SW, which are subparallel to S_{Hmax} in the Western Canada Sedimentary Basin, are likely to be more resistant to closure than those oriented NW-SE, parallel to S_{Hmin} trajectories. Local exceptions exist, particularly in the Rocky Mountain Foothills, where there are indications of open fractures running NW-SE, parallel to thrust planes and fold axes (Barss and Montandon, 1981).

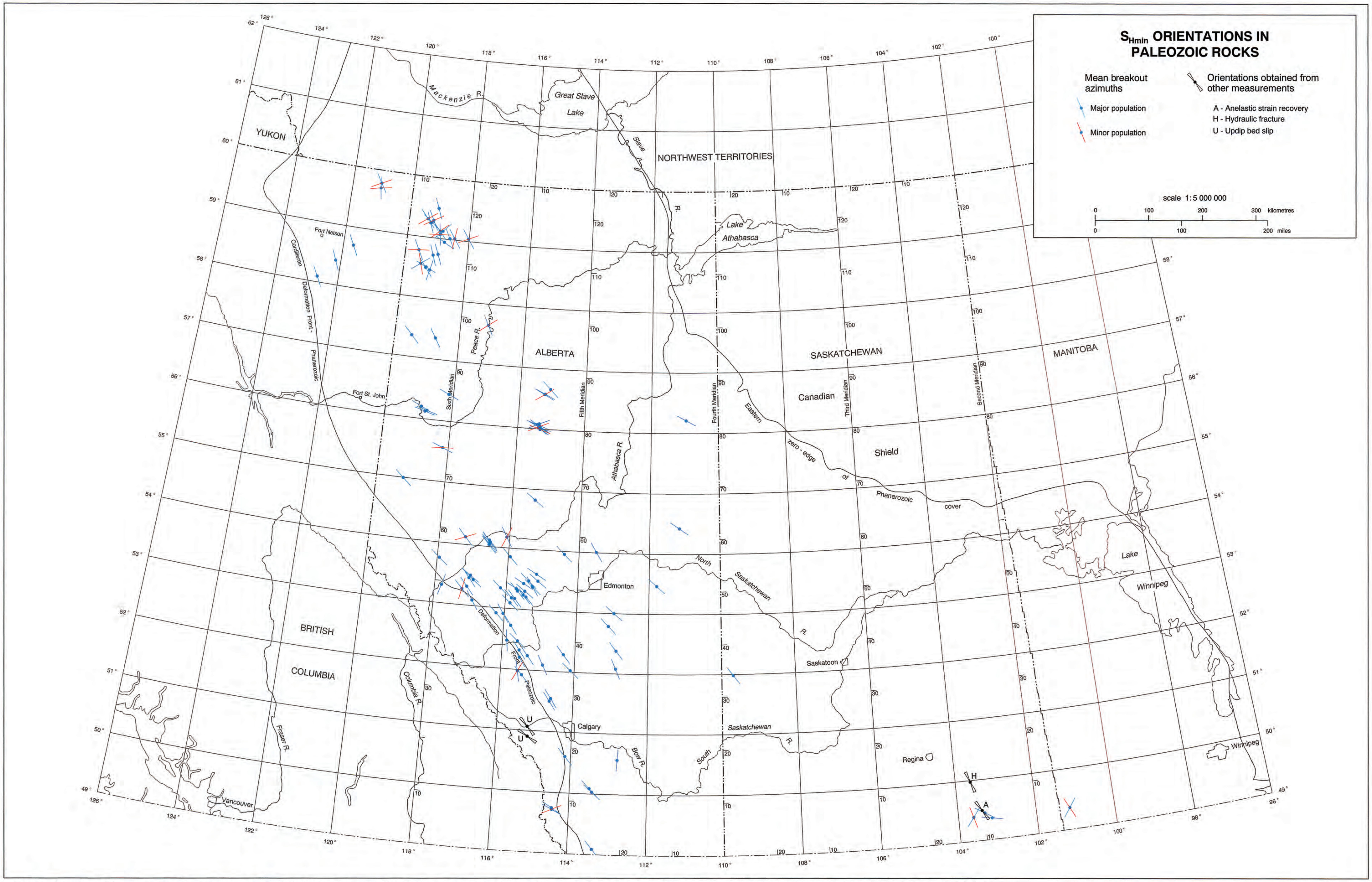

Figure 29.8 Orientations of S_{Hmin} measured in Paleozoic rocks in the Western Canada Sedimentary Basin. The majority of orientations are derived from mean well azimuths of breakouts (Table 29.3). Other stress orientation indicators (Table 29.4) are also shown.

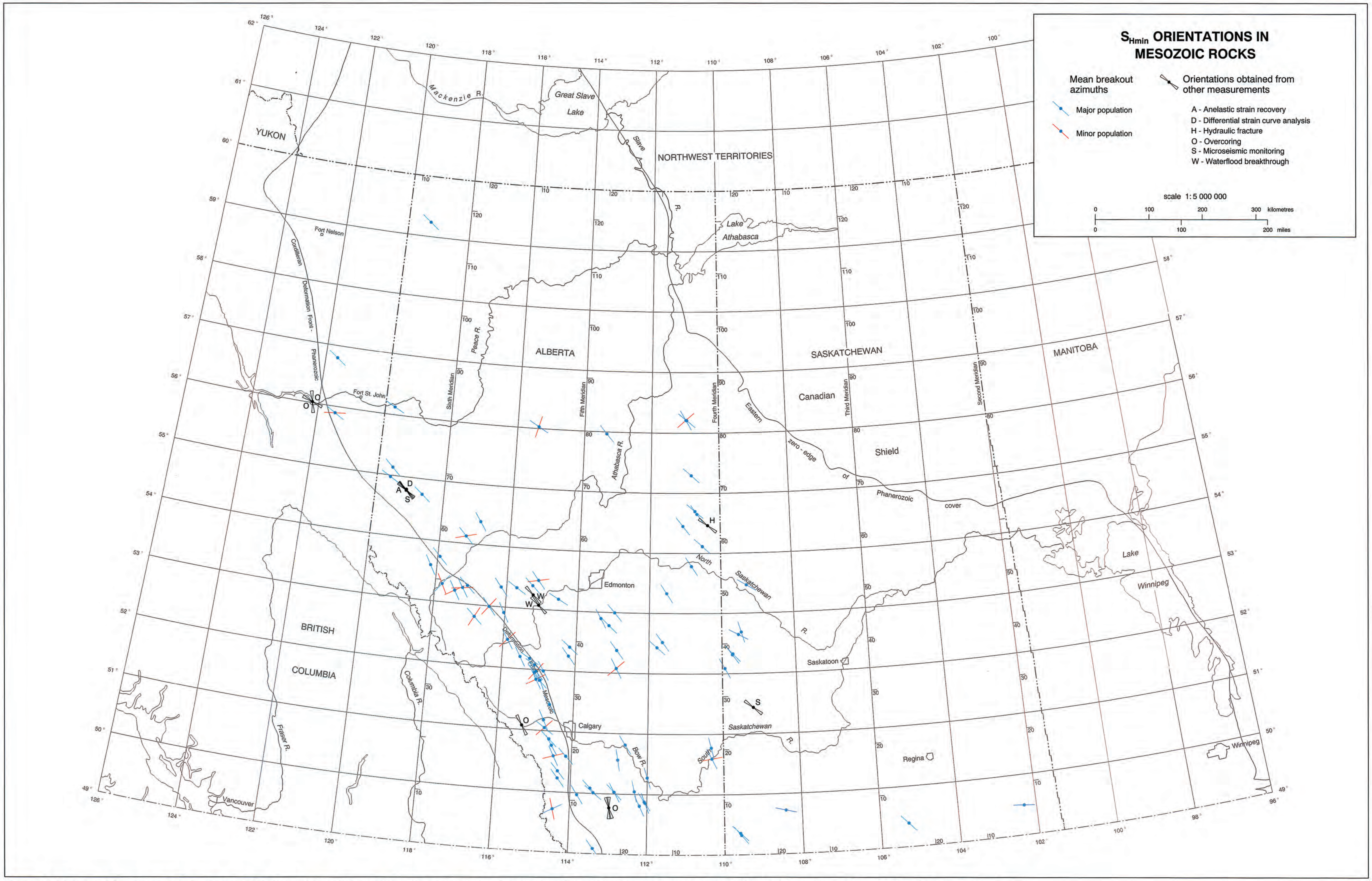

Figure 29.9 Orientations of S_{Hmin} measured in Mesozoic rocks in the Western Canada Sedimentary Basin. The majority of orientations are derived from mean well azimuths of breakouts (Table 29.3). Other stress orientation indicators (Table 29.4) are also shown.

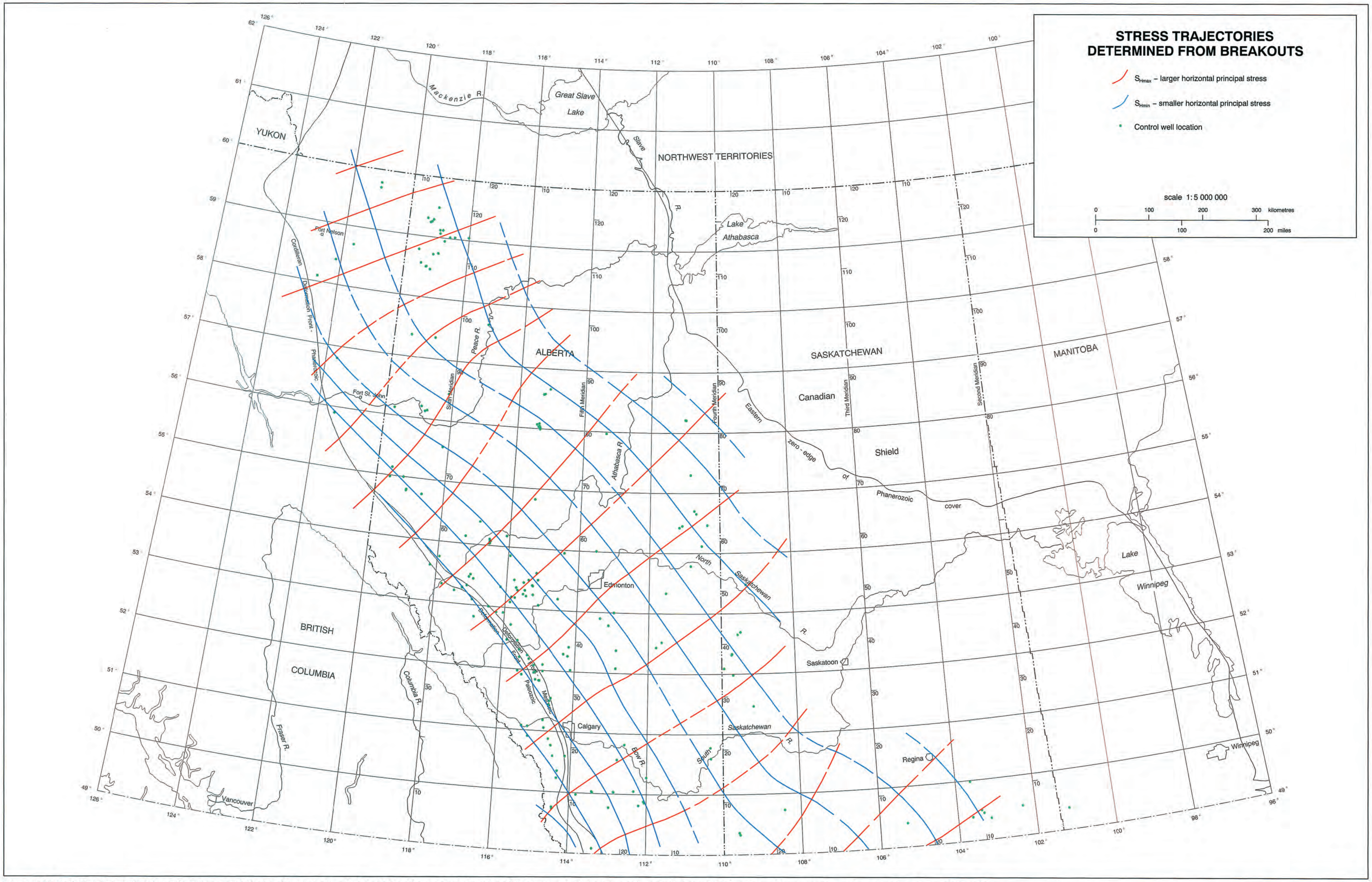

Figure 29.10 Horizontal stress trajectories projected across the Western Canada Sedimentary Basin. The interpretation is based on all the measured principal stress orientation indicators in Paleozoic and Mesozoic rocks, as documented on Figures 29.8 and 29.9.

Table 29.4 S_{Hmax} orientations measured in the Western Canada Sedimentary Basin by methods other than breakout analysis. Locations are shown on Figures 29.8 and 29.9.

Geographic location/well	Location	Measurement method	Depth in m	S_{Hmax} (std. dev.)	Comments	Reference
Canmore	51.072°N, 115.351°W	Overcoring	240	55.0°-66.0°	Coal mine roof	Grant, 1970
Pembina oil field "J"Lease	53.233°N, 115.250°W	Waterflood breakthrough	1615	c.45.0°	Well connections due to waterflooding	McLeod, 1977
Cold Lake	54.460°N, 110.363°W	Hydraulic fracture	457	30.0°-45.0°		Imperial Oil, 1978
Kipp Mine	49.768°N, 112.977°W	Overcoring Overcoring	152 180	c.90.0° 70.0° (20.0°)		Kaiser et al., 1982
Pembina oil field "F"Lease	53.067°N, 115.083°W	Waterflood breakthrough	1675	c.45.0°	Well connections due to waterflooding	Hassan, 1982
Exshaw	51.065°N, 115.187°W	Updip bed slip	Surface	49.0°		Bell, 1985
Kananaskis valley	50.903°N, 115.170°W	Updip bed slip	Surface	32.0°		Bell, 1985
3-8-12-12W2	49.977°N, 103.611°W	Hydraulic fracture Hydraulic fracture	2065 2168	70.0° 71.0°	Packer impression Packer impression	McLennan et al., 1986
2b-11-67-8W6	54.779°N, 119.103°W	Anelastic strain recovery Differential strain curve analysis Microseismic monitoring	1227-1260 1227-1260	35.5° (17.2°) 42.8° (14.7°) 35.0° (15.0°)	 Fracture propagation directions sensed	McLellan, 1988
C9-23-6-11W2	49.491°N, 103.383°W	Anelastic strain recovery	1407	59.0°	Range: 55.0°-70.0°	McLellan et al., 1991
W.A.C. Bennett Dam	56.016°N, 122.196°W 56.014°N, 122.194°W	Overcoring Overcoring	137 137	20.0° 76.0°	Averaged azimuth Averaged azimuth	Imrie, 1991
10-28-28-24W3	51.426°N, 109.316°W	Microseismic monitoring	705	52.0°	Fracture propagation directions sensed	Talebi et al., 1991

On a continent-wide scale, the Western Canada Sedimentary Basin lies within the North American Mid-Plate Stress Province, which is characterized by NE-SW-trending S_{Hmax} orientations (Zoback and Zoback, 1980; Adams and Bell, 1991). Mean S_{Hmax} azimuths measured in the Western Canadian Sedimentary Basin, and at many locations within the Mid-Plate Stress Province (Zoback et al., 1989), coincide closely with the absolute plate motion vectors determined for the North American Plate (Minster and Jordan, 1978). This suggests that the horizontal stress anisotropy documented in the sediments may be an upper crustal manifestation of mantle drag on the base of the lithosphere. For Western Canada, the basal drag could be exerted by the lithosphere sliding southwestward across the asthenosphere (Zoback and Zoback, 1980), or by northeastward sublithospheric mantle flow, as proposed by Gough (1984). Bell et al. (1992) have noted that the directional coincidence of plate motion vectors and S_{Hmax} orientations appears to be most pronounced in the faster moving plates.

Acknowledgements

The authors thank their respective employers for permission to publish this chapter. J.D. McLennan, H.S. Chhina and L. Vandamme are thanked for providing information to supplement their published stress measurements. Unpublished formation leak-off test data were supplied by the Energy Resources Conservation Board of Alberta. The authors are grateful for the critical reviews of P.R. Kry, I. Shetsen and G.S. Stockmal, which have led to significant improvements in this chapter.

References

Adams, J. and Bell, J.S. 1991. Crustal stresses in Canada. *In:* Neotectonics of North American. D.B. Slemmons, E.R. Engdahl, M.D. Zoback and D.D. Blackwell (eds.). Geological Society of America, Decade Map Volume, p. 367-386.

Barss, D.L. and Montandon, F.A. 1981. Sukunka-Bullmoose gas fields: models for a developing trend in the southern Foothills of northeast British Columbia. Bulletin of Canadian Petroleum Geology, v. 29, p. 293-333.

Bell, J.S. 1985. Offset boreholes in the Rocky Mountains of Alberta, Canada. Geology, v. 13, p. 734-737.

Bell. J. S. 1990. Investigating stress regimes in sedimentary basins using information from oil industry wireline logs and drilling records. *In:* Geological Applications of Wireline Logs. A. Hurst, M. A. Lovell and A. C. Morton (eds.). Geological Society of London, Special Publication 48, p. 305-325.

Bell, J. S. and Babcock, E. A. 1986. The stress regime of the Western Canadian Basin and implications for hydrocarbon production. Bulletin of Canadian Petroleum Geology, v. 34, p. 364-378.

Bell, J. S., Caillet, G., and Adams J. 1992. Detection of open fractures and non-sealing faults with dipmeter logs. *In:* Geological Applications of Wireline Logs II. A.C. Hurst, C.M. Griffiths, and P.F. Worthington (eds.). Geological Society Special Publication 66, p. 211-220.

Bell, J. S. and Gough, D. I. 1979. Northeast-southwest compressive stress in Alberta: evidence from oil wells. Earth and Planetary Science Letters, v. 45, p. 475-482.

Bell, J. S. and McCallum, R. E. 1990. In situ stress in the Peace River Arch area, Western Canada. Bulletin of Canadian Petroleum Geology, v. 38A, p. 270-281.

Bell, J. S. and Price, P. R. 1989. In-situ stresses in Western Canada - Implications for the oil industry (Poster). Geological Survey of Canada Oil and Gas Forum, Calgary, Feb 27-28, 1989.

Breckels, I.M. and Van Eekelen, H.A.M. 1981. Relationship between horizontal stress and depth in sedimentary basins. Paper SPE 10336, 56th Annual Fall Technical Conference, Society of Petroleum Engineers of AIME, San Antonio, Texas, October 5-7, 1981.

Ervine, W.B. and Bell, J.S. 1987. Subsurface in-situ stress magnitudes from oil well drilling records: an example from the Venture area, offshore Eastern Canada. Canadian Journal of Earth Sciences, v. 24, p. 1748-1759.

Gough, D.I. 1984. Mantle upflow under North America and plate dynamics. Nature, v. 311, p. 428-433.

Grant, F. 1970. Roof stability in coal mines: investigations at Wilson Mine. Canmore Mines Ltd., Internal Report MR70/21-ID, Mining Research Centre, Mines Branch, Energy, Mines and Resources Canada, 55 p.

Gronseth, J.M. 1990. Geomechanics monitoring of cyclic steam simulation operations in the Clearwater formation. *In:* Rock at Great Depth. V. Maury and D. Fourmaintraux (eds.). v. 3, p. 1393-1398, Balkema, Rotterdam.

Hassan, D. 1982. A method for predicting hydraulic fracture azimuth and the implication thereof to improve hydrocarbon recovery. Paper 82-33-19, 33rd Annual Technical Meeting, Petroleum Society of The Canadian Institute of Mining and Metallurgy, Calgary, June 6-9, 1982.

Hoek, E. and Brown, E.T. 1980. Underground Excavations in Rock. Institute of Mining and Metallurgy, London, 527 p.

Hobbs, B.E. and Talbot, J. L. 1966. The analysis of strain in deformed rocks. Journal of Geology, v. 74, p. 500-513.

Holzhausen, G.R., Wood, M.D., Raisbeck, J.M. and Card, C.C. 1980. Results of deformation monitoring during steam stimulation during a single-well test. Paper presented at the Applied Oil Sands Geoscience Conference, Edmonton, Canada, 1980.

Hubbert, M.K. and Willis, D.G. 1957. Mechanics of hydraulic fracturing. Petroleum Transactions (AIME), v. 210, p. 153-166.

Imperial Oil. 1978. The Cold Lake Project. Report to Energy Resources Conservation Board of Alberta.

Imrie, A.S. 1991. Stress-induced response from both natural and construction-related processes in the deepening of the Peace River valley, B.C. Canadian Geotechnical Journal, v. 28, p. 719-728.

Jaeger, J.C. and Cook, N.G.W. 1979. Fundamentals of Rock Mechanics. 3rd Edition, London. Chapman and Hall.

Kaiser, P.K., Mackay, C. and Morgenstern, N. R. 1982. Performance of a shaft in weak rock (Bearpaw Shale). *In:* Rock Mechanics: Caverns and Pressure Shafts. W. Wittke (ed.). Proceedings, International Society of Rock Mechanics Symposium, Aachen.

Kry, P.R. and Gronseth, J.M. 1983. In-situ stresses and hydraulic fracturing in the Deep Basin. Journal of Canadian Petroleum Technology, November-December 1983 Issue, p. 31-36.

Leshchyshyn, T.H. and Seyer, W.G. 1990. Three field techniques to estimate the effective permeability and fracture properties of Athabasca Oil Sands. Paper 53-24 presented at the International Technical Meeting of the Petroleum Society of CIM and the Society of Petroleum Engineers, Calgary, June 10-13, 1990.

McLellan, P.J. 1988a. In-situ stress prediction and measurement by hydraulic fracturing, Wapiti, Alberta. Journal of Canadian Petroleum Technology, v. 27, no. 2, p. 85-95.

McLellan, P.J. 1988b. In-situ stress magnitudes from hydraulic fracture treatment records - a feasibility study. Geological Survey of Canada, Open file Report 1947, 30 p.

McLellan, P.J., Lawrence, K., and Cormier K. 1992. A multiple-zone acid stimulation treatment of a horizontal well, Midale, Saskatchewen. Journal of Canadian Petroleum Technology, v. 31, no. 4, p. 71-82.

McLeod J.G.F. 1977. Sucessful injection pattern alteration, Pembina J lease, Alberta. 28th Annual Meeting of the Petroleum Society of the Canadian Institute of Mining, Edmonton, Alberta, Paper.

McLennan, J.D., Elbel, J., Mattheis, E. and Lindstrom, L. 1982. A critical evaluation of the mechanical properties log (MPL) on a basal quartz well in the Caroline area. Paper 82-33-45, 33rd Annual Technical Meeting of the Petroleum Society of the Canadian Institute of Mining and Metallurgy, Calgary, June 6-9, 1982.

McLennan, J.D., Hasegawa, H.S., Roegiers, J-C. and Jessop, A.M. 1986. Hydraulic fracturing experiment at the University of Regina Campus. Canadian Geotechnical Journal, v. 23, p. 548-555.

Minster, J.B. and Jordan, T.H. 1978. Present-day plate motions. Journal of Geophysical Research, v. 83, p. 5331-5354.

Proskin, S.A., Scott, J.D., and Chhina, H. S. 1990a. Interpretation of the minimum stress from micro-frac tests. *In:* Rock at Great Depth. V. Maury and D. Fourmaintraux (eds.). v. 3, p. 1509-1519, A. A. Balkema, Rotterdam.

Proskin, S.A., Scott, J.D., and Chhina, H. S. 1990b. Current practice in the interpretation of microfrac tests. Paper SPE 20040, presented at the 60th California Regional Meeting of the Society of Professional Engineers, Ventura, California, U.S.A., April 4-6, 1990.

Salz, L.B. 1977. Relationship between fracture propagation pressure and pore pressure. Paper SPE 6870, presented at the 1977 Society of Petroleum Engineers' Annual Technical Conference and Exhibition, Denver, U. S. A., October 7-12, 1977.

Settari, A. and Raisbeck, J. M. 1978. Fracture mechanics analysis in in-situ oil sands recovery. Paper 78-29-18, 29th Annual Technical meeting of the Petroleum Society of the Canadian Institute of Mining and Metallurgy, Calgary, June 13-16, 1978.

Talebi, S., Young, P.R., Vandamme, L., and McGanghey, W.J. 1991. Microseismic mapping of a hydraulic fracture. *In:* Rock Mechanics as a Multidisciplinary Science. J-C Roegiers (ed.). A.A. Balkema, Rotterdam, P. 461-470.

Woodland, D.C. and Bell, J. S. 1989. In-situ stress magnitudes from mini-frac records in Western Canada. Journal of Canadian Petroleum Technology, v. 28, p. 22-31.

Wyman, R. E., Holdich, S. A., and Randolph, P.L. 1980. Analysis of an Elmworth hydraulic fracture in Alberta. Journal of Petroleum Technology, v. 32, p. 1621-1630.

Zoback, M.L. and Zoback, M.D. 1980. State of stress in the conterminous United States. Journal of Geophysical Research, v. 85, p. 6113-6156.

Zoback, M.L. et al. 1989. Global patterns of tectonic stress. Nature, v. 341, p. 291-298.